

MASTER

IMPLEMENTATION OF A NONEQUILIBRIUM CONDENSATION
MODEL IN RELAP4/MOD7

S. R. Fischer, H. Chow, G. Van Arsdall
EG&G Idaho, Inc.
Idaho Falls, Idaho 83401

H. Stadtke
J.R.C.
Ispra, Italy

NOTICE
This report was prepared as an account of work sponsored by the United States Government. Neither the United States nor the United States Department of Energy, nor any of their employees, nor any of their contractors, subcontractors, or their employees, makes any warranty, express or implied, or assumes any legal liability or responsibility for the accuracy, completeness or usefulness of any information, apparatus, product or process disclosed, or represents that its use would not infringe privately owned rights.

RELAP4^{1,2}, which is used to simulate the thermal hydraulic behavior of light water reactors subjected to various LOCA transients, is based on the assumption of thermodynamic equilibrium between liquid and vapor within fluid volumes. This assumption, while being appropriate for much of a LOCA transient, is not adequate during the ECC accumulator injection phase as determined by comparisons of code calculations with experimental data. To overcome this limitation, a general model to simulate the nonequilibrium phenomena associated with the mixing of subcooled water with saturated steam has been developed and is operational on preliminary versions of RELAP4/MOD7.

Incorporation of this nonequilibrium condensation model into RELAP4 required the addition of a separate explicit liquid energy balance to the RELAP4 equation set. This explicit approach, using previous time step information, was taken so as to facilitate implementation within the basic RELAP4 framework and to minimize computation time. Condensation rates are computed for each fluid volume using a simple flow regime dependent constitutive package. Correlations for interphase heat and mass transfer rates for the bubble flow and dispersed flow regimes are included. Wall heat transfer and net vaporization in subcooled boiling are also considered.

Preliminary versions of the nonequilibrium mixing model have been used to perform calculations of Westinghouse cold leg ECC injection tests³ and Battelle ECC bypass tests⁴. Comparisons between RELAP4/MOD7 code simulations of these facilities and experimental measurements have indicated the need for considering nonequilibrium effects in code simulations of LOCA transients. In addition, the results indicate the need for continued development of constitutive relations for use in modeling steam-water mixing interactions. Further assessment of the nonequilibrium condensation model performance will be carried out prior to the public release of RELAP4/MOD7 through the National Energy Software Center, Argonne, Illinois.

IMPLEMENTATION OF A NONEQUILIBRIUM CONDENSATION MODEL IN RELAP4/MOD7

INTRODUCTION

RELAP4¹ is a computer code which has been written specifically to analyze the thermal hydraulic behavior of light water nuclear reactors subjected to various postulated LOCA type transients. The code is quite general in nature and thus can be used to analyze the two-phase flow and heat transfer characteristics of various experimental blowdown and reflood facilities. RELAP4/MOD6² is the current publically released version of the code and is available through the National Energy Software Center at Argonne, Illinois and the OECD/NEA Computer Program Library in Paris.

The basic RELAP4 code provides for the solution of the time-dependent one-dimensional conservation of mass, momentum and energy equations written for fluid control volumes. The basic code assumes homogeneous fluid conditions and thermodynamic equilibrium between phases within a control volume. Special models have in recent years been incorporated within the basic code framework to relax or remove some of the homogeneous equilibrium assumptions for special circumstances; that is, formation of a well-defined mixture level, superheating of vapor during reflood or slip between liquid and vapor phases in gravity dominated flow. The addition of these non-homogeneous or nonequilibrium models to the RELAP4 code has greatly improved the capability of the code to predict the complex thermohydraulic phenomena occurring during the blowdown, refill, and reflood phases of a postulated LOCA in a light water reactor.

One of the major model development efforts associated with RELAP4/MOD7 is the development and implementation of a nonequilibrium condensation model. The prime motivation for this development effort is the need for a calculational model for the refill phase of a postulated LOCA. The thermal equilibrium assumption inherent in the basic RELAP4 code is neither adequate nor suitable during the ECC accumulator injection phase of a LOCA transient. The homogeneous assumption implies that subcooled ECC water mixes instantly with steam. This process rapidly depressurizes the fluid volume due to steam condensation which occurs as a result of the equilibrium fluid state achieved each time step. The assumption of thermal equilibrium during ECC injection has been the cause of numerous code calculational problems including water packing, pressure oscillations, increased run time and inconsistent code-data comparisons.

Allowing saturated steam and subcooled water to coexist, and limiting the condensation rate through physical considerations can have a large influence on the depressurization rate of a reactor during a LOCA. This pressure change will in turn affect the ECC bypass process in a PWR thereby

impacting the refill behavior of the reactor downcomer and lower plenum. The temperature of the water delivered to the lower plenum that later enters the core during the reflood phase of a LOCA transient plays an important role in the reflood process. For instance, experimental results from LOFT⁵ indicate that water delivered to the lower plenum can be substantially subcooled.

The present nonequilibrium condensation model development effort is restricted to dealing with the thermal nonequilibrium of two-phase steam-water mixtures where the departure from equilibrium is associated only with subcooling of the liquid phase. That is, the present model addresses physical situations such as that occurring during ECC injection when subcooled water mixes with saturated or nearly saturated steam. This mixing of subcooled water with steam occurs not only in the cold leg injection section of a PWR but also in the downcomer during periods of reverse core steam flow. The present model is expected to be applicable or useful for the analysis of PWR upper head injection or hot leg injection systems and for BWR spray systems. During the upper head spray cooling phase of a hypothetical BWR LOCA, condensation of steam on subcooled water droplets may play an important role in determining water delivery to the reactor core. Nonequilibrium occurring in these situations is assumed, for the present model, to approach an equilibrium state through interface heat and mass transfer processes (condensation) between phases.

Nonequilibrium condensation models have been incorporated into several of the advanced system and component LOCA codes such as TRAC⁶, K-TIF⁷, RELAP5⁸, and DRUFAN⁹. Other nonequilibrium models have been discussed and proposed by Saha¹⁰, Jones and Saha¹¹, and Hughes et al¹². These models are, for the most part, based on simple empirical type correlations relating a condensation rate J and liquid thermal nonequilibrium $T_s - T_l$, that is

$$J \sim (T_s - T_l)$$

Wolfert⁹ and Hughes¹² attempt to calculate the condensation rate by computing meaningful interfacial areas and heat transfer coefficients based on flow regime considerations. DRUFAN⁹ utilizes simple correlations for bubbly flow at low void fractions ($\alpha < 0.3$) and for dispersed flow at high void fractions ($\alpha > 0.7$). Condensation rates at intermediate void fractions are apparently determined through interpolation. Hughes et al¹² recommends a somewhat more complex set of correlations for interfacial area and heat transfer coefficients.

One major drawback of these nonequilibrium condensation models is that they all require specification of empirical constants which must be determined through comparisons of code calculations with experimental data. Clearly, such simplistic models can not be expected to be universally applicable to all of the mixing situations likely to occur during reactor transients. Enhanced mixing resulting from turbulence, fluid interactions with reactor internals, liquid injection techniques, and pipe roughness should ideally be taken into account. With the present state of knowledge, only an approximation to the physical situation can be anticipated.

In this paper the standard RELAP4 equilibrium assumptions will be reviewed, the proposed nonequilibrium model will be discussed, the unique scheme used to implement the nonequilibrium model in the RELAP4 framework will be presented and finally results of code calculations made using the new model will be compared with experimental data.

RELAP4 EQUILIBRIUM CONSIDERATIONS

In the RELAP4 ^{1,2} code the thermohydraulic behavior of a system is described by mass and energy conservation equations for each control volume and by one-dimensional momentum balances written across the interfaces (junctions) between control volumes. The determination of the thermodynamic state of the fluid within a control volume is based on the following assumptions:

(1) Homogeneous fluid conditions exist provided phase separation models are not applied

(2) The flow of fluid is one-dimensional through volumes and across junctions

(3) For two-phase mixtures, $0 < x < 1.0$, pressure equilibrium exists between phases

$$p_g = p_l = p$$

(4) For two-phase mixtures, $0 < x < 1.0$, temperature equilibrium exists between phases

$$T_g = T_l = T_s$$

(5) For single-phase volumes subcooled or superheated conditions can be obtained. For $x_e \leq 0.0$, $T_l \leq T$ or for $x_e \geq 1.0$, $T_g \geq T_s$.

For a control volume $V(i)$, RELAP4 uses the total volume mass $M(i)$ and fluid internal energy $U(i)$ as independent variables from which to determine the fluid state.

Using Figure 1 for reference, the conservation equations for mass and energy can be written (neglecting potential and kinetic energy terms and assuming no air present) as:

$$\dot{M}(i) = \sum_{j, \text{in}} [w_g(j) + w_l(j)] - \sum_{j, \text{out}} [w_g(j) + w_l(j)] \quad (1)$$

$$\dot{U}(i) = \sum_{j, \text{in}} [w_g(j) h_g(j) + w_l(j) h_l(j)] - \sum_{j, \text{out}} [w_g(j) h_g(j) + w_l(j) h_l(j)] + Q_{\text{wall}}(i) \quad (2)$$

$$\dot{V}(i) = 0 \quad (3)$$

From the specific volume $v(i) = \frac{V(i)}{M(i)}$ and specific internal energy $u(i) = \frac{U(i)}{M(i)}$ all other thermodynamic quantities can be determined based on the equilibrium assumptions. Mass and energy transfer between phases are implied by the equilibrium conditions. When subcooled water is injected into a volume containing a two-phase mixture an equilibrium fluid state is obtained which for two-phase conditions implies that the injected liquid instantly reaches saturation independent of the injection rate, the degree of subcooling and the volume conditions. This process results in unrealistically high depressurization rates.

NONEQUILIBRIUM CONDENSATION MODEL

The primary purpose of the nonequilibrium condensation model is to allow the coexistence of saturated steam and subcooled liquid within a single control volume. This coexistence implies that the heat and mass transfer rate between phases is no longer determined only by mass and energy conservation principles. An additional constitutive equation is necessary to calculate the condensation rate depending on the extent of the departure from equilibrium.

The main assumptions for the nonequilibrium model can be summarized as follows:

(1) The distribution of each phase is homogeneous throughout the fluid volume implying complete mixing of incoming fluid with fluid already present in the volume.

(2) For two-phase mixtures pressure equilibrium is assumed between phases

$$P_g = P_l = p.$$

(3) For two-phase mixtures, the vapor phase is always assumed to be at saturation conditions

$$T_g = T_s = T(p).$$

(4) The liquid phase may be subcooled. The degree of subcooling is determined in part by the mass and energy transfer between phases.

(5) The condensation rate is governed by the degree of subcooling, the interfacial area and an interfacial heat transfer coefficient.

The last assumption leads to the following expression for the mass of vapor which condenses per unit time, $\dot{M}_{COND}(i)$,

$$\dot{M}_{COND}(i) = \frac{h_i(i) A_i(i) [T_s(i) - T_l(i)] V(i)}{h_{gs}(i) - h_{ls}(i)} \quad (4)$$

To predict the thermodynamic properties of each phase in a nonequilibrium system, separate mass and energy balances are needed for each phase. Using Figure 2 for reference, the mass and energy balances can be written as:

$$\dot{M}_g(i) = \sum_{j,in} w_g(j) - \sum_{j,out} w_g(j) - \dot{M}_{COND}(i) \quad (5)$$

$$\dot{M}_l(i) = \sum_{j,in} w_l(j) - \sum_{j,out} w_l(j) + \dot{M}_{COND}(i) \quad (6)$$

$$\begin{aligned} \dot{U}_g(i) = \sum_{j,in} w_g(j) h_g(j) - \sum_{j,out} w_g(j) h_g(j) + \dot{Q}_g(i) \\ - p(i) \dot{V}_g(i) - \dot{M}_{COND}(i) h_g(i) \end{aligned} \quad (7)$$

$$\begin{aligned} \dot{U}_l(i) = \sum_{j,in} w_l(j) h_l(j) - \sum_{j,out} w_l(j) h_l(j) + \dot{Q}_l(i) \\ - p(i) \dot{V}_l(i) + \dot{M}_{COND}(i) h_g(i) \end{aligned} \quad (8)$$

In general, the total wall heat transfer $\dot{Q}_{wall}(i)$ can be thought of as composed of two terms, $\dot{Q}_l(i)$ and $\dot{Q}_g(i)$, such that $\dot{Q}_{wall}(i) = \dot{Q}_l(i) + \dot{Q}_g(i)$.

Additional equations are necessary to determine the wall heat transfer depending on wall temperature and fluid conditions. Also, the constant volume assumption in RELAP4 yields

$$\dot{V}(i) = \dot{V}_g(i) + \dot{V}_l(i) = 0 \quad (9)$$

and the state equation for saturated vapor and subcooled liquid

$$(u_g, h_g, v_g, s_g) = f(p) \quad (10)$$

$$(u_l, h_l, v_l, s_l) = f(T_l, p)$$

With Equations 4 through 10, a complete set of differential equations has been obtained to describe the thermal nonequilibrium conditions in a control volume. An implicit implementation of these equations into RELAP4 would require a completely different solution technique than is presently used. Therefore, to expedite implementation and minimize changes to the existing code, the following method has been chosen to interface the nonequilibrium condensation model with the RELAP4 equation set.

IMPLEMENTATION SCHEME

The nonequilibrium situation (saturated vapor coexisting with subcooled liquid) is replaced with an equivalent equilibrium system by introducing a pseudo heat input to a volume $Q^*(i)$ and a pseudo work, $p^*(i) \dot{V}^*(i)$, done by the fluid in the volume. This equivalent control volume is shown in Figure 3. The terms $p^*(i) \dot{V}^*(i)$, and $Q^*(i)$ have to be chosen in such a manner that the equivalent equilibrium system will result in the same depressurization rate, $\dot{p}(i)$, and the same condensation rate, $\dot{M}_{COND}(i)$, as the true nonequilibrium system expressed by Equations 4 through 10. That is,

$$\begin{aligned} \dot{M}_{COND}^*(i) &= \dot{M}_{COND}(i) \\ \dot{p}^*(i) &= \dot{p}(i) \end{aligned} \quad (12)$$

Using Figure 3 for reference, the overall conservation equations for the equivalent equilibrium system can be written as follows:

$$\dot{V}^*(i) \neq 0$$

$$\dot{M}^*(i) = \sum_{j,in} [w_g(j) + w_l(j)] - \sum_{j,out} [w_g(j) + w_l(j)] \quad (13)$$

$$\begin{aligned} \dot{U}^*(i) &= \sum_{j,in} [w_g(j) h_g^*(j) + w_l(j) h_l^*(j)] - \\ &\quad \sum_{j,out} [w_g(j) h_g^*(j) + w_l(j) h_l^*(j)] + \\ &\quad Q^*(i) - p^*(i) \dot{V}^*(i) \end{aligned} \quad (14)$$

The equations for the pseudo heat input $Q^*(i)$ and the pseudo volume expansion rate $\dot{V}^*(i)$ can be derived by equating the equivalent equilibrium system with the real nonequilibrium case using the conditions given by Equation (12).

$$\begin{aligned} Q^*(i) &= -\dot{M}_{COND}(i) [h_g^*(i) - h_l^*(i)] - \sum_{j,in} w_g(j) [h_g^*(j) - h_g^*(i)] \\ &\quad - \sum_{j,in} w_l(j) [h_l^*(j) - h_l^*(i)] + \sum_{j,out} w_g(j) [h_g^*(j) - h_g^*(i)] \\ &\quad + \sum_{j,out} w_l(j) [h_l^*(j) - h_l^*(i)] + \\ &\quad [M_g^* T_g^* \left(\frac{ds_g}{dp}\right)^* + M_l^* T_l^* \left(\frac{ds_l}{dp}\right)^*]_i \dot{p}(i) \end{aligned} \quad (15)$$

$$\begin{aligned} \dot{V}^*(i) = & \sum_{j,in} [w_g(j) v_g^*(i) + w_l(j) v_l^*(i)] - \sum_{j,out} [w_g(j) v_g^*(i) \\ & + w_l(j) v_l^*(i)] - \dot{M}_{COND}(i) [v_g^*(i) - v_l^*(i)] + [M_g^* \left(\frac{dv_g}{dp}\right)^* \\ & + M_l^* \left(\frac{dv_l}{dp}\right)^*]_i \dot{p}(i) \end{aligned} \quad (16)$$

where

$\dot{M}_{COND}(i)$ is given in Equation 4 and $\dot{p}(i)$ can be derived from Equations 5 through 10.

The thermal nonequilibrium situation differs from the base equilibrium case in RELAP4 by an additional term in the overall energy equation, $[\dot{Q}(i) - \dot{p}^*(i) \dot{V}^*(i)]$, and two additional differential equations for the volume size, $\dot{V}^*(i)$ [Equation (16)], and the enthalpy of the liquid phase $H_l(i)$. If the new values for $\dot{V}^*(i)$, $\dot{M}^*(i)$, $\dot{U}^*(i)$ and $H_l(i)$ are known, all other thermodynamic quantities can be determined from the corresponding specific values:

$$v^*(i) = \frac{V^*(i)}{M^*(i)}, \quad u^*(i) = \frac{U^*(i)}{M^*(i)}, \quad h_l(i) = \frac{H_l(i)}{M_l(i)}$$

Pressure, vapor quality and the state variables of the saturated vapor phase are calculated as in the above equilibrium case:

$$[p(i), x(i), h_g^*(i), s_g^*(i), v_g^*(i)] = f[v^*(i), u^*(i)]$$

The state of the subcooled liquid, however, is obtained from the state equations of the liquid phase:

$$[T_l(i), h_l(i), s_l(i), u_l(i)] = f[h_l(i), p(i)]$$

The relatively complex equations for the liquid enthalpy, the pseudo heat input, and the pseudo volume expansion rate can be considerably simplified by additional assumptions concerning the state of the fluid in the control volume.

During the refill phase of a blowdown, the pressure differences in the coolant system are relatively small. Because the specific enthalpy of the saturated vapor is only a function of the pressure, we can assume that the differences in the specific enthalpies between adjacent volumes are small compared with other terms in the energy equation:

$$\sum_{j,in} h_g^*(j) - h_g^*(i) \approx 0$$

$$\sum_{j,out} h_g^*(j) - h_g^*(i) \approx 0$$

For two-phase states with void fractions not too close to zero, the compressibility of the two-phase mixture is governed by the compressibility of the vapor phase. For this condition, a constant liquid density can be assumed.

$$\left[\left(\frac{\partial v_l}{\partial p} \right)_T \right]_{(i)} \approx 0, \quad \left[\left(\frac{\partial v_l}{\partial T} \right)_p \right]_{(i)} \approx 0 \quad \text{and} \quad v_l(i) \approx v_l^*(i)$$

If the pressure term in the energy equation for the liquid phase as well as for the overall two-phase mixture is assumed small relative to the condensation term, then

$$\begin{aligned} \dot{H}_l(i) = & \sum_{j, \text{in}} w_l(j) h_l(j) - \sum_{j, \text{out}} w_l(j) h_l(j) + \dot{Q}_{\text{wall}}(i) \\ & + \dot{M}_{\text{COND}}(i) h_g(i) \end{aligned} \quad (17)$$

$$\dot{V}^*(i) = 0$$

$$\begin{aligned} U^*(i) = & \sum_{j, \text{in}} [w_g(j) h_g^*(i) + w_l(j) h_l^*(i)] - \sum_{j, \text{out}} [w_g(j) h_g^*(i) \\ & + w_l(j) h_l^*(i)] - \dot{M}_{\text{COND}}(i) [h_g^*(i) - h_l^*(i)] \end{aligned} \quad (18)$$

These equations are used in the implementation of the nonequilibrium condensation model in the RELAP4/MOD7 code. The overall equilibrium energy balance given by Equation 2 is modified for the nonequilibrium calculation to yield Equation 18. A separate explicit liquid energy balance [Equation 17] is performed for each nonequilibrium volume to keep track of the total liquid enthalpy.

CONSTITUTIVE RELATIONS FOR INTERFACIAL HEAT TRANSFER

The energy transfer between subcooled liquid and saturated vapor is calculated as indicated in Equation 4 by computing interfacial heat transfer coefficients and appropriate interfacial areas. In the present model, simple expressions are determined for $h_i(i)$ and $A_i(i)$ for bubble flow and dispersed droplet flow. The bubble and dispersed flow regimes are specified through knowledge of mass flux G and void fraction α as shown in Figure 4. The flow map in Figure 4 resulted from simplifying the modified Bennett¹³ vertical flow regime map. An interpolation scheme is used to obtain the $h_i(i)$ $A_i(i)$ term across the transition region.

For bubbly flow the rate of bubble collapse is assumed to be governed by the convection of latent heat away from the vapor-liquid interface and into the liquid phase. Assuming spherical bubbles of uniform sizes, the interfacial heat transfer coefficient and interfacial area can be expressed as shown in references 12-16 as:

$$h_i(i)_{\text{bubble}} = \left[\frac{2 v_r k_l \rho_l c_{pl}}{\pi r_b} \right]^{1/2}$$

$$A_i(i)_{\text{bubble}} = \frac{3\alpha}{r_b}$$

For dispersed flow, with liquid droplets uniformly distributed in a continuous saturated vapor phase, the condensation rate is assumed to be controlled by the conduction of latent heat from the droplet surface into the droplet bulk. For spherical droplets with uniform diameters the heat conduction into the droplet bulk is given in Reference 6 as:

$$h_i(i)_{\text{drop}} = 8.067 \frac{k_l}{r_d}$$

The corresponding interfacial area for dispersed flow is:

$$A_i(i)_{\text{drop}} = \frac{3(1-\alpha)}{r_d}$$

The bubble radius r_b and droplet radius r_d are computed based on a Weber number criterion using Zuber's churn turbulent drift expression ¹⁷ with a critical Weber number of:

$$We_{\text{CRIT}} = 8.0 \text{ for bubbly flow }^{16} \text{ and}$$

$$We_{\text{CRIT}} = 12.0 \text{ for dispersed droplet flow }^{18}.$$

In the transition region for $10^5 < G < 10^6$, a two-point interpolation technique is employed. For $G > 10^6$, a three-point interpolation procedure is used to prevent discontinuities across flow regime boundaries.

NONEQUILIBRIUM MODEL EVALUATION

A preliminary evaluation of the RELAP4/MOD7 nonequilibrium condensation model has been conducted using the Battelle 1/15-scale transparent vessel PWR tests ⁴ and Westinghouse 1/3-scale cold leg ECC injection ³ results as data bases. These experimental results were used to determine the effectiveness of the nonequilibrium model in describing nonequilibrium refill phenomena. Within RELAP4/MOD7 the nonequilibrium condensation model is used in conjunction with the RELAP4 slip model to account for refill behavior incident to a PWR LOCA. Therefore, to evaluate the model required not only an understanding of system refill and pressure response, but also the interfacial heat transfer. Both the Battelle and Westinghouse results provided indicators of the importance of the nonequilibrium effect through measurement of liquid temperatures.

The Battelle facility, Figure 5, is a 1/15-scale transparent model of a PWR designed to explore the effects of ECC subcooling, ECC flow rate, and various reverse core steam flows on refill of a four-loop reactor. The system consists of three intact blind flanged cold legs with corresponding ECC injectors, an extended lower plenum allowing for more complete definition of filling rate, and a simulated containment. During a typical test, a reverse core steam flow was established through the system and allowed to equilibrate prior to injection of the ECC water. For each test, various system pressures, flow rates, and fluid temperatures along with the plenum refill rate are monitored.

To simulate the Battelle facility the RELAP4/MOD7 model shown in Figure 6 was developed. The model consisted of a seven-volume, eight junction system with the three intact cold legs lumped into a single volume, two downcomer volumes centered about respective thermocouples, and a time-dependent volume simulating containment. A newly implemented flow regime dependent slip model was specified for all downcomer junctions along with complete phase separation in the lower plenum. Thermal nonequilibrium was assumed for all volumes except the simulated core and containment. The model was initialized by impressing a given reverse core steam flow on an initially atmospheric stagnant system. When the system equilibrated, the ECC injection ramp was initiated.

Comparisons of RELAP4 calculations with experimental results from Battelle Test No. 8, shown in Figures 7 to 9, are indicative of the type of results obtained in simulation of high penetration, high ECC subcooling experiments. Figure 7 indicates that not only is the RELAP4 computed refill in agreement with the data, but the initiation of delivery is within acceptable data limits. To arrive at this comparison, a sequential ECC injection into the cold legs was assumed. This assumption was based on observations of similar sequential drops in the intact cold leg fluid temperatures. Note that the RELAP4 simulation yields a time averaged delivery rate in contrast to the periodic slug delivery evidenced in the data.

Figures 8 and 9 further compliment the Test 8 comparison. In Figure 8, the computed plenum pressure is observed to fall within the band widths of the highly oscillatory data. As may be noted, the pressure prediction is well within a time averaged range. The calculated downcomer (Volume 2) liquid temperature is compared with a fluid temperature measurement in Figure 9. As clearly indicated, the RELAP4 model appears to have reasonably well accounted for the nonequilibrium mixing phenomena.

In Table 1 the results of RELAP4 simulations of several other Battelle tests are compared with experimental data. Results for lower plenum pressure, average lower plenum refill rate and downcomer liquid temperatures are compared. The experimental testssimulated represent the refill spectrum from low penetration or high bypass tests (Test No. 3), to medium penetration tests (Test No. 2) and finally to high penetration tests (Test Nos. 1,8). For all of the tests, the injected ECC water was about 40F which represented the most severe test of the nonequilibrium condensation model. As indicated by the comparisons given in Table 1, the calculated refill rates, plenum pressure and downcomer liquid temperature agree reasonably well with the experimental measurements.

To gain further insight into the effectiveness of the nonequilibrium model, the Westinghouse 1/3-scale experiments were explored. In these tests a 1/3-scale simulated PWR cold leg, Figure 10, was connected between large surge tanks. For the test, superheated steam was supplied to the upstream surge tank creating a flow through the test section. The system was allowed to equilibrate at which time subcooled ECC water was injected through the injection nozzle. As in the Battelle test, fluid temperatures and pressures were recorded for a matrix of steam and water injection rates, liquid subcooling, and system pressures.

Figure 11 is the RELAP model employed for the Westinghouse analysis. It consisted of 25 volumes and 26 junctions. The outlet surge tank was simulated by a time-dependent volume. Two fill junctions were employed, one connected to the inlet flow chamber accommodated the steam flow and the other simulated the ECC injection flow. During a typical run, steam was first introduced into the system and allowed to equilibrate before the water was injected.

Comparisons between RELAP4 calculations and experimental data for two Westinghouse SIS injection tests are presented in Figures 12 and 13. In Figure 12 the calculated liquid temperature agrees quite well with the measured data for the low flow high subcooling injection Test 5-57. Substantial mixing of water and steam occurs in the immediate vicinity of the injection section rapidly bringing the water to saturation. In Figure 13 the agreement between calculated and measured temperatures for Test 5-32 is again quite good. For this high injection rate run, substantial mixing occurs for several pipe diameters downstream of the injection region in the RELAP4 model as evidenced by the distance required for the liquid to reach saturation. The experimental temperatures indicate more condensation in the immediate injection region than computed by the nonequilibrium model.

CONCLUSION

A general model to simulate the nonequilibrium phenomena associated with the mixing of subcooled water with saturated water has been developed and is operational on preliminary versions of RELAP4/MOD7. Initial assessment of the model using Battelle ECC bypass test data and Westinghouse cold leg ECC injection data has yielded encouraging results. Comparisons between RELAP4 calculations and experimental data for the Westinghouse tests indicate that the nonequilibrium condensation model predicts the trends of the experimental data reasonably well. The experimental data indicates a very high mixing rate in the immediate vicinity (within one pipe diameter) of the injection section. The RELAP4 calculation indicates that the mixing process occurs over a much longer distance (\approx 8 to 10 pipe diameters) downstream of the injection section. Enhanced mixing, which is not accounted for in the RELAP4 model, occurs in the injection section due to increased turbulence. Properly accounting for this enhanced mixing points out the difficulty in establishing constitutive relations for interfacial heat transfer and areas that are universally applicable.

The results of the simulations of the Battelle facility indicate that the nonequilibrium model with the RELAP4 slip model can be used to predict

refill type phenomena. Comparisons between code calculations and experimental data for high, medium and low penetration tests with cold ECC water (40F) were encouraging. The measured downcomer fluid temperatures compared favorably with the calculated liquid temperatures indicating again that the nonequilibrium model constitutive package is yielding condensation rates consistent with test data.

Additional code simulations of the Battelle⁴ and Creare¹⁹ ECC bypass tests and the LOFT⁵ and Semiscale²⁰ system tests are planned and needed to provide further assessment of the nonequilibrium condensation model.

NOMENCLATURE

A	-	area per unit volume
c_p	-	specific heat at constant pressure
c_v	-	specific heat at constant volume
D_h	-	hydraulic diameter
G	-	mass flux
h_i	-	interfacial heat transfer coefficient
h	-	specific enthalpy
H	-	total enthalpy
h_{fg}	-	latent heat of vaporization
J	-	condensation rate/unit volume
k	-	thermal conductivity
M	-	mass
\dot{M}_{COND}	-	condensation rate
p	-	pressure
\dot{Q}_{wall}	-	wall heat transfer
\dot{Q}_i	-	wall heat transfer into phase i
r	-	radius
s	-	specific entropy
T	-	temperature
U	-	total internal energy
u	-	specific internal energy

V - volume of fluid cell
v - specific volume
w - mass flow rate
x - quality
 α - void fraction
 ρ - density

SUBSCRIPTS

g - vapor
l - liquid
s - saturation
i - interfacial
b - bubble
d - droplet

SUPERSCRIPTS

* - refers to an equivalent equilibrium value for a nonequilibrium quantity
. - derivative with respect to time

ARGUMENTS

j - junction value
i - volume quantity

REFERENCES

- 1 K. R. Katsma et al, RELAP4/MOD5 - A Computer Program for Transient Thermal Hydraulic Analysis of Nuclear Reactors and Related Systems, Vols. I, II, III, ANCR-NUREG-1335 (1976).
- 2 S. R. Fischer et al, RELAP4/MOD6 - A Computer Program for Transient Thermal Hydraulic Analysis of Nuclear Reactors and Related Systems, User's Manual, CDAP-TR-003, EG&G Idaho, Inc. (January 1978). Available through the National Energy Software Center, Argonne, Illinois.
- 3 G. R. Lilly, L. E. Hochreiter, Mixing of Emergency Core Cooling Water with Steam: 1/3-Scale Test and Summary, EPRI 294-2 Final Report (June 1975).

- 4 R. A. Cudnik et al, Penetration Behavior in a 1/15-Scale Model of a Four-Loop Pressurized Water Reactor, BMI-NUREG-1073, NRC-2 (June 1977).
- 5 D. L. Batt, Experiment Data Report for LOFT Nonnuclear Test Ll-4, TREE-NUREG-1084 (July 1977).
- 6 TRAC-PIA - An Advanced Best-Estimate Computer Program for PWR LOCA Analysis, NUREG CR-0063, LA-7279-MS, Vol. 1 (June 1978).
- 7 A. A. Amsden and F. H. Harlow, K-TIF: A Two-Fluid Computer Program for Downcomer Flow Dynamics, LA-6994, NRC-4 (January 1978).
- 8 V. H. Ransom et al, RELAP5 Code Description, CDAP-TR-78-035, EG&G Idaho, Inc., Internal Report (August 1978).
- 9 K. Wolfert, "The Simulation of Blowdown Processes with Condensation of Thermodynamic Nonequilibrium Phenomena," Specialists Meeting on Transient Two-Phase Flow sponsored by the OECD/Nuclear Energy Agency, Toronto, Canada, August 3-4, 1976.
- 10 P. Saha, "Direct Contact Condensation," Reactor Safety Research Programs Quarterly Progress Report (October 1 - December 31, 1977), BNL-NUREG-50785 (February 1978), pp 198-203.
- 11 O. C. Jones and P. Saha, "Nonequilibrium Aspects of Water Reactor Safety," Thermal and Hydraulic Aspects of Nuclear Reactor Safety, Vol. 1: Light Water Reactors, O. C. Jones and S. G. Bankoff (eds.), ASME (1977), pp 249-288.
- 12 E. D. Hughton et al, An Evaluation of State-of-the-Art Two-Velocity, Two-Phase Flow Models and Their Applicability to Nuclear Reactor Transient Analysis, EPRI NP-143 (February 1976).
- 13 A. W. Bennett, G. F. Hewitt et al, Flow Visualization Studies of Boiling at High Pressure, AERE-R-4874 (1967).
- 14 E. Rukenstein, "On Heat Transfer Between Vapor Bubbles in Motion and the Boiling Liquid from Which They are Generated," Chem. Eng. Sci. 10, 22 (195).
- 15 D. Moalem and S. Sideman, "The Effect of Motion on Bubble Collapse," Int. J. Heat Mass Transfer, 16, 2321 (1973).
- 16 M. Ishii, One-Dimensional Drift-Flux Model and Constitutive Equations for Relative Motion Between Phases in Various Two-Phase Flow Regimes, ANL-77-47 (1977).
- 17 N. Zuber and J. A. Findlay, "Average Volumetric Concentration in Two-Phase Flow System," J. Heat Transfer 87, 453 (1965).
- 18 E. O. Moeck, Annular-Dispersed Two-Phase Flow and Critical Heat Flux, AECL-3656.

- 19 C. J. Crowley et al, Downcomer Effects in a 1/15-Scale PWR Geometry - Experimental Data Report, NUREG-0281, NRC-2 (May 1977).
- 20 B. L. Collins et al, Experiment Data Report for Semiscale MOD-3 Blowdown Heat Transfer Test S-07-1 (Baseline Test Series), NUREG/CR-0281, also TREE-1221 (September 1978).

Figure 1. Control Volume for Mass and Energy Balance (Equilibrium Case)

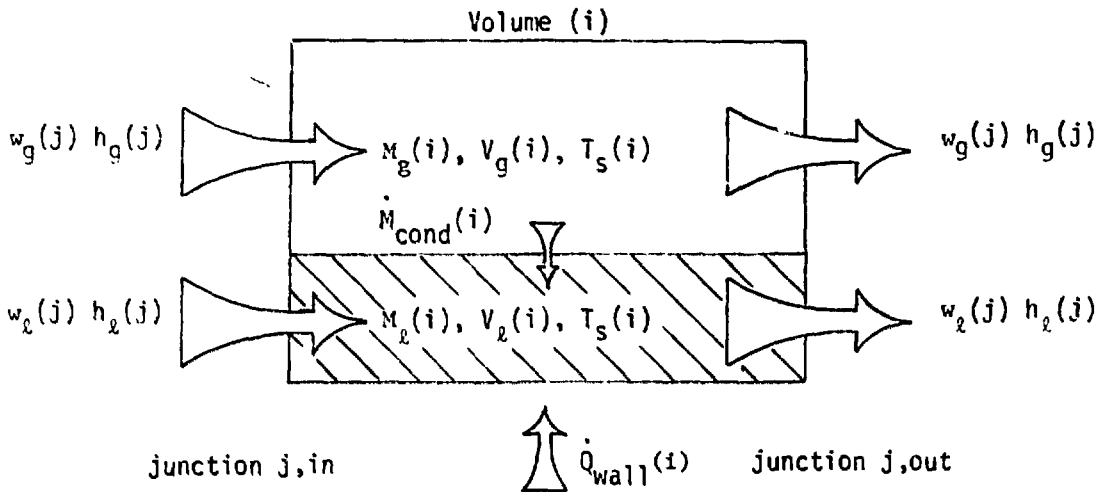


Figure 2. Control Volume for Mass and Energy Balance (Nonequilibrium Case)

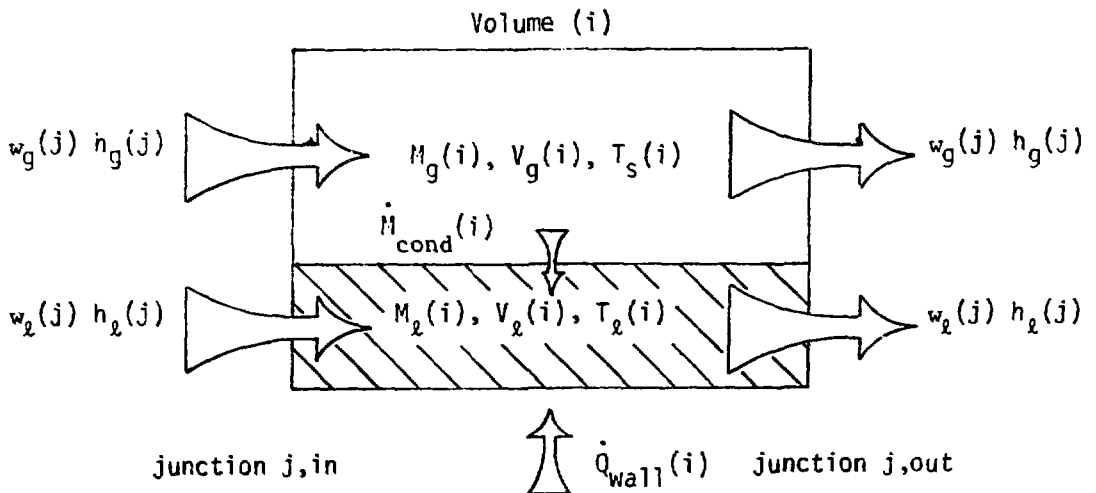


Figure 3. Equivalent Equilibrium System; Same Conditions as in Figure 2 Except That the Liquid Phase is Saturated

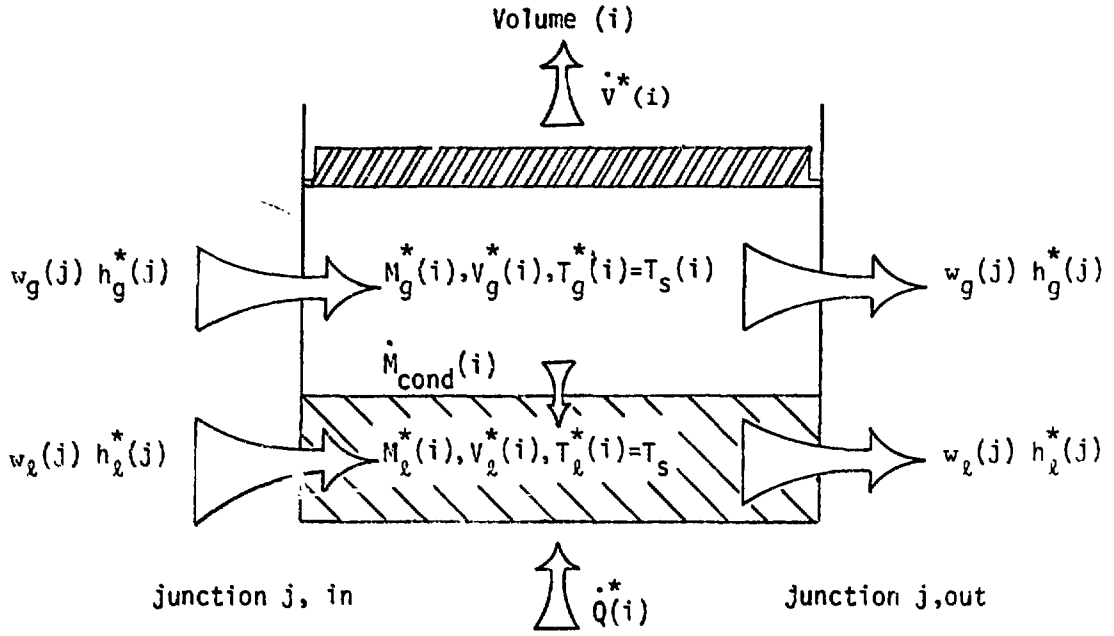
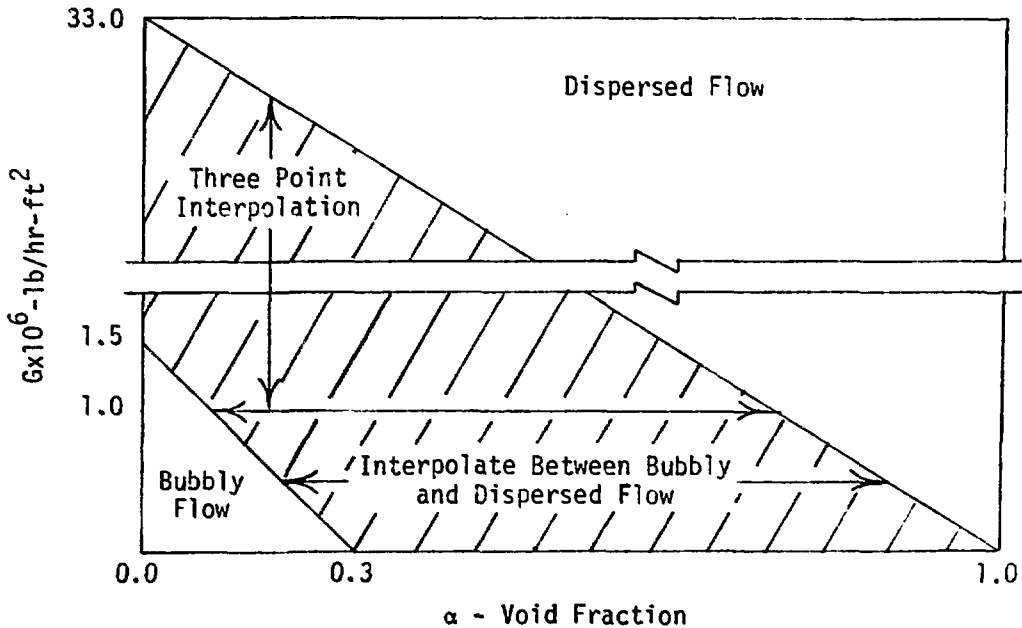


Figure 4. Flow Region Map



For $G < 10^5$, G is set equal to 10^5

Figure 5. Schematic of BCL 1/15-Scale Facility

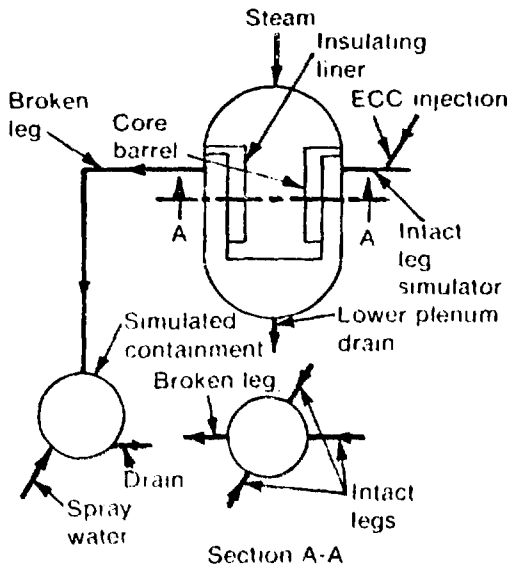
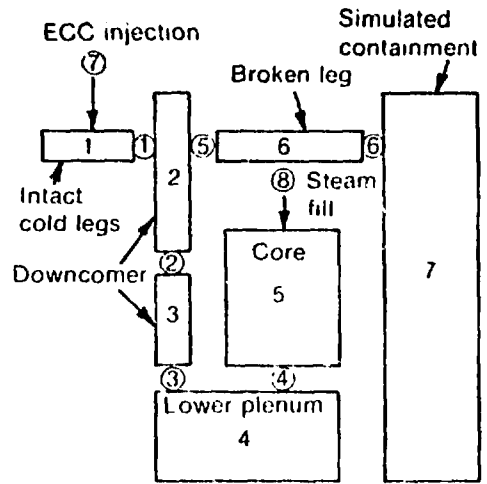


Figure 6. RELAP Model of BCL 1/15-Scale Facility



Note.

- 1) Volume numbers denoted by uncircled integers
- 2) Junction numbers denoted by circled integers

Figure 7. Battelle Test No. 8 Lower Plenum Refill Comparison

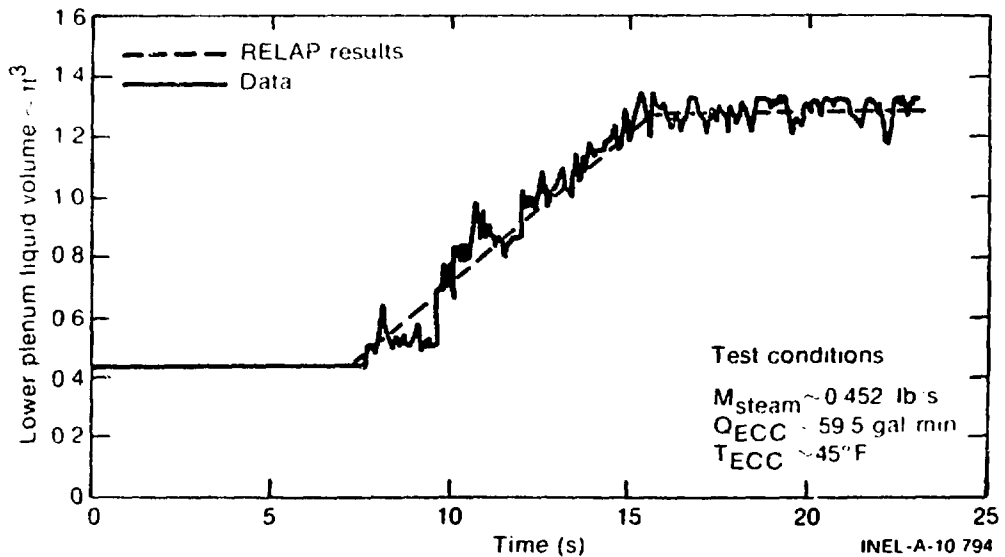


Figure 8. Battelle Test No. 8 Lower Plenum Pressure Comparison

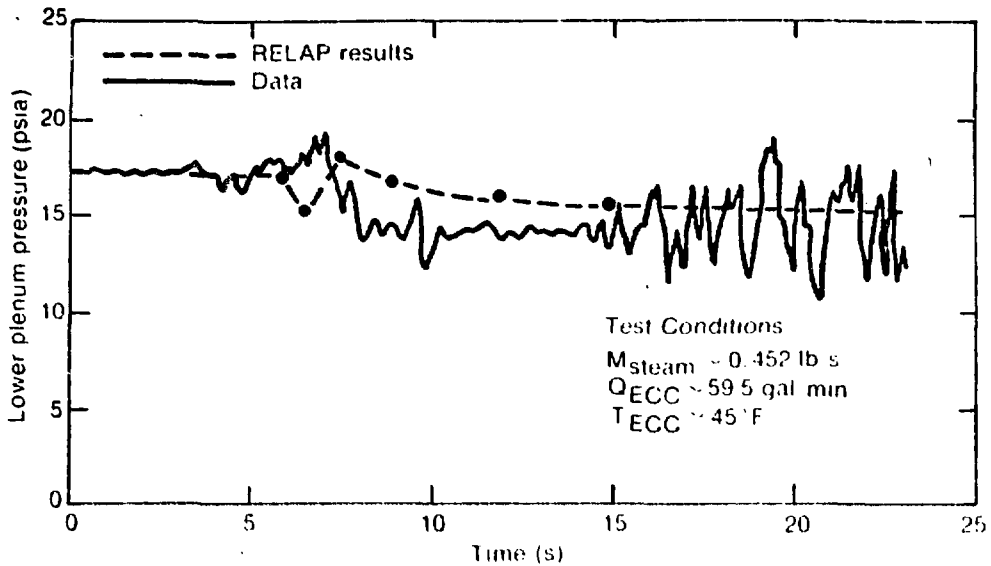


Figure 9. Battelle Test No. 8 Downcomer Liquid Temperature Comparison

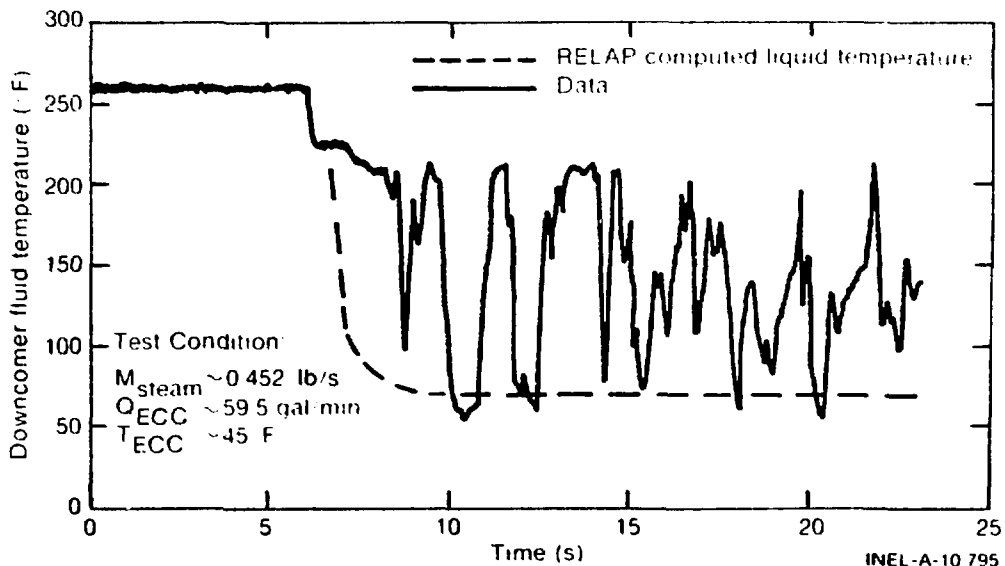


Table 1. Result Comparisons for 1/15-Scale Battelle Test

Test no.	Steam flow lb/sec	ECC flow gal./min	ECC temp F	Plenum pressure psia		Refill rate ft ³ /sec		Downcomer temperature F	
				Test ^a	RELAP	Test	RELAP	Test ^b	RELAP
				1	2.14	29.3	45.	14.0-17.3	19.6
2	2.84	28.8	43.	14.2-17.8	19.7	.040	.034	93.-146.	91.
3	3.34	28.9	44.	14.1-23.4	23.5	.012	.020	101.-149.	95.
8	2.51	59.5	45.	12.5-17.6	16.5	.117	.095	56.-98.	71.

^aRange of pressure oscillations.

^bCircumferential liquid temperature range.

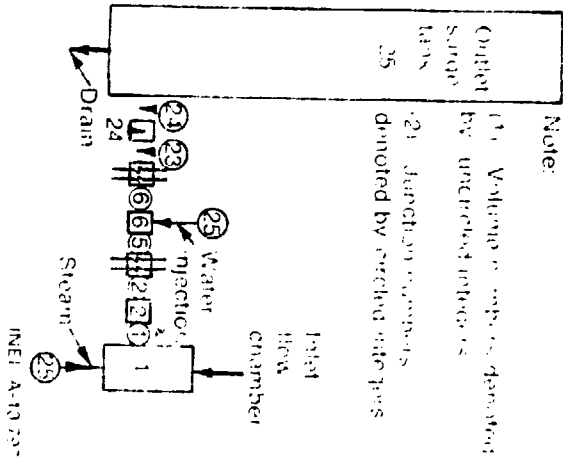


Figure 11. RELAP Model of Westinghouse 1/3-Scale Facility

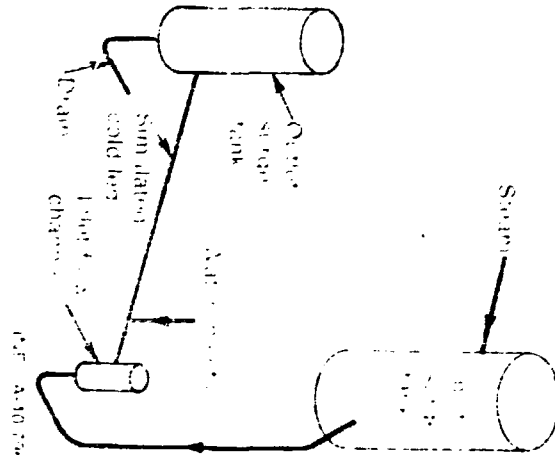


Figure 10. Schematic of Westinghouse 1/3-Scale Facility

Figure 12. Westinghouse 1/3-Scale Cold Leg Liquid Temperature Comparison (Run No. 5-57-1)

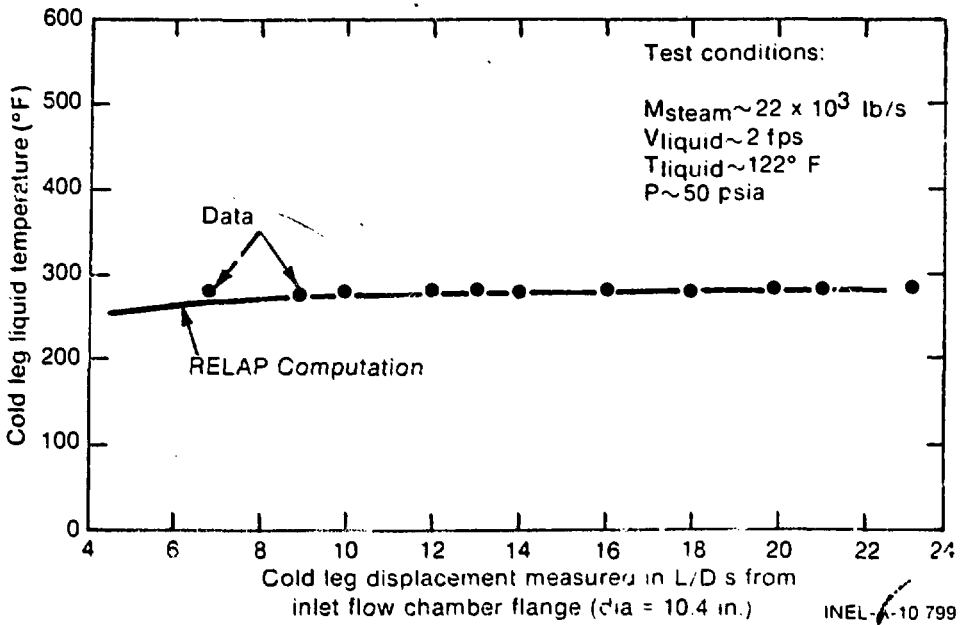


Figure 13. Westinghouse 1/3-Scale Cold Leg Liquid Temperature Comparison (Run No. 5-32)

